Heliyon 10 (2024) e27866

Contents lists available at ScienceDirect

Heliyon

journal homepage: www.cell.com/heliyon

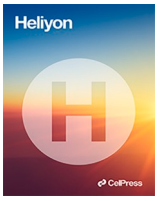

Research article

Delayed luminescence to monitor growth stages and assess the entropy of *Saccharomyces cerevisiae*

Qing Li *, Hong Wu, Miao Tian, Danyu Li, Peng Zheng, Xiaochun Zhang, Bruce Qing Tang

ENNOVA Institute of Life Science & Technology, ENN Group, Langfang 065001, China

ARTICLE INFO

Keywords:
Delayed luminescence
Saccharomyces cerevisiae
DL emission parameter
Growth stages
Entropy

ABSTRACT

Delayed luminescence (DL) refers to the photon-induced ultra-weak luminescence emitted by samples after the light source is switched off. As a noninvasive method for health monitoring and disease diagnosis, DL has attracted increasing attention. The further development of this technology is valuable for the study of complex biological processes, such as different growth stages. If such studies were to be conducted in humans, large numbers of subjects of all ages would need to be recruited, and individual differences would be inevitable. The budding yeast *Saccharomyces cerevisiae* (*S. cerevisiae*) has a short population lifespan, and the growth phases can be monitored within dozens of hours. Therefore, *S. cerevisiae* is an ideal model organism for research. In this study, we investigated the physiological characteristics and DL emission of *S. cerevisiae* during growth in glucose-based media and entry into stationary phase, and the results showed that DL kinetic curves of yeast cells in the growing phase were obviously separated from those of stationary phase cells. Moreover, the metabolic and physiological characteristics of the yeast cell population were discussed using the DL emission parameters I_0, τ and γ. We also discussed the possibility of assessing entropy using DL emission parameters. Our research demonstrates the potential of this technology to be used in wider applications.

1. Introduction

Recently, increasing attention has been focused on the possibility of using noninvasive methods in health monitoring and disease diagnosis. Among the various possible detection methods, there is growing interest in the use of delayed luminescence (DL). DL is a widespread photon-induced ultraweak luminescence phenomenon that is emitted by many samples for a long time after the light source is switched off (usually on a microsecond to second time scale) [1,2]. Activated by light irradiance, molecules in biological systems absorb light energy and form many different electronic excited states. Molecules in high energy states are unstable and easily transit back to low energy states and release energy to form DL emission.

DL was first observed in plant samples by Strehler and Arnold [3] and later in other biological samples, such as leaves [4], chloroplasts [5], and photosynthetic bacteria [6]. With the development of relevant technology, DL spectroscopy has been applied for the detection of human cells [7,8], tissues [9,10] and acupuncture points in the human body [9]. Although the origin of DL is still not clear, it is generally believed that DL can reflect some basic properties and biochemical reactions of biological systems to an extent. In

* Corresponding author. ENNOVA Institute of Life Science & Technology, No.118, Huaxiang Road, Langfang 065001, Hebei, China.
E-mail address: liqinga@enn.cn (Q. Li).

https://doi.org/10.1016/j.heliyon.2024.e27866
Received 31 July 2023; Received in revised form 1 March 2024; Accepted 7 March 2024
Available online 22 March 2024

many studies, the application of DL has shown the possibility of distinguishing tumor cells and normal cells [10–13]. In other studies, DL has been used to monitor cell apoptosis [14,15] or to assess the pro-apoptotic capacity of combined cancer treatments [16]. Researchers have also explored the utilization of DL as a screening tool to assess a person's acute or chronic disease status as a whole [17,18].

According to the second law of thermodynamics, the entropy of a closed system tends toward a maximum. It was not until the 1950s that entropy began to gain prevalence in discussions of living phenomena. The entropy generation approach has been used to evaluate the stationary states of cells in relation to the global results of cell biophysical and biochemical processes [19]. Entropy is a measure of the disorder of a system and shows that more disorder means higher entropy content. Gu infers that the DL parameter τ is related to the order degree of a biosystem, which can characterize its entropy [20]. On this basis, it would be very meaningful to extend DL technology to analyze more complicated biological processes, such as different growth stages in the lifespan.

There are many difficulties that would need to be overcome if such studies were conducted in humans, such as recruiting large numbers of subjects of all ages and accommodating for the inevitable individual differences. In this context, the budding yeast *Saccharomyces cerevisiae* (*S. cerevisiae*) has been deemed a suitable model organism for this research because it has a short population lifespan, and growth stages can be monitored within dozens of hours. The growth phases of *S. cerevisiae* cells growing on glucose-based media include the initial logarithmic phase, the 'diauxic shift' phase, the subsequent postdiauxic phase, and the stationary phase after the external nutrients are exhausted [21,22]. During the growth period (before entering the stationary phase), the yeast cells go through different metabolic modes as the carbon source changes. Meanwhile, in some studies, yeast was proposed to be a sensitive and versatile model system that could be used for further study of DL [23,24]. Therefore, we used the yeast *S. cerevisiae* as a model organism for related research, such as using DL to detect oxidative stress in yeast cells [25], and demonstrated that DL can be used as an indicator of mitochondrial status under different glucose supply conditions [26].

In this study, we used DL to monitor certain growth stages of *S. cerevisiae* growing on glucose-based media and analyzed the metabolic and physiological characteristics of the yeast cell population using the DL emission parameters I_0, τ and γ.

2. Materials and methods

2.1. Yeast strain and growth conditions

The industrial instant dry yeast *S. cerevisiae* (Angel Yeast CO. Ltd., China) was used in this study. This commercial yeast strain has been isolated and purified by multigeneration monoclonal cloning; it is a fast-growing, vigorous and stable strain and has been previously used in many experiments in our laboratory [25–27]. The yeast cells were cultured to logarithmic phase in YPD medium (1% yeast extract, 2% tryptone, and 2% D- (+)-glucose), and a certain number of yeast cells were harvested and stored in a refrigerator at 4 °C for more than 24 h before use. To shorten the experiment time, the medium was diluted to 1/4 YPD, i.e., three parts of sterile water were added to one part of YPD as the medium for the experiment. After recovery at 25 °C for 0.5 h, the yeast cells were inoculated with 1/4 YPD at a final concentration of 1×10^7 cells/mL. After culturing at 30 °C with rotational shaking at 160 rpm for 0, 2, 4, 6, 24, 48 and 72 h, the yeast cells were collected for further detection. To avoid errors introduced by different batches of measurement, yeasts cultured for different times were collected and tested at the same time. The cell number of the samples was measured with a blood cell counting plate. All reagents were purchased from Sigma–Aldrich (Steinheim, Germany). All glassware and medium were autoclaved at 121 °C for 20 min. Each experiment was performed three times.

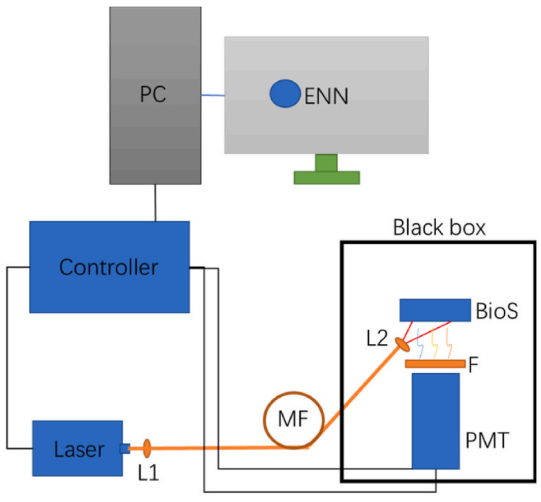

Fig. 1. Schematic diagram of the delayed luminescence acquisition system. MF: Multimode optical fiber, PMT: Photomultiplier tube, BioS: biological sample, L1/L2: Lens, F: Filter.

2.2. Delayed luminescence measurement

The measurement of DL from cell cultures was performed using the installed equipment shown in Fig. 1. The PC is connected to the circuit controller via a USB port to deliver commands and collect data through software written by the ENN group. The laser emitted 405 nm light, which passed through a lens (L1), a multimode fiber (MF) and a lens (L2) to adjust the beam size and irradiate the biological sample (BioS). Then, the DL emission is received by a photomultiplier tube (PMT) (CR104, Hamamatsu, China) in single photon counting mode and transmitted back to the PC through the circuit controller. The circuit controller developed by the ENN group controlled the laser and PMT switches within microsecond accuracy. To protect PMT from photon oversaturation, a filter (F) was added between the BioS and the PMT, which attenuated the photon by 50%.

To prevent possible photobleaching and/or photodamage, the cell density and laser intensity were optimized. Our preliminary data indicated that DL had a linear relationship with cell density at 1-4 $\times$ 10^8 cells/mL. In this study, 2 $\times$ 10^8 cells/mL were collected by rapid centrifugation, washed twice, resuspended in PBS (phosphate-buffered saline) and loaded directly into a quartz colorimetric cuvette with an optical diameter of 1 mm. After being fixed in a black circular holder with a 12 mm diameter hole on the bottom, the sample was illuminated by 20 mW laser light, and the DL emission was measured. At the same time, an equal volume of PBS was loaded into the quartz colorimetric cuvette and measured to discuss the DL from their own. The laser excitation time was 10 ms, and then signals were initially collected after 4 ms of laser excitation. In an acquisition time of 80 ms, the controller collected data every 1.6 ms, i.e., photoemission was recorded between 4 and 84 ms after laser excitation.

2.3. High-performance liquid chromatography analysis for adenosine triphosphate (ATP)

The ATP content in yeast cells was determined by high-performance liquid chromatography (HPLC) as described by Sumi et al. with modifications [28]. Briefly, a fraction of the sample was transferred to Eppendorf tubes and centrifuged at 10,000 rpm and 4 °C for 5 min. The sediment was treated with 360 μL of 6% perchloric acid solution (sigma) at 0 °C for 10 min and then centrifuged at 10,000 rpm and 4 °C for 5 min to precipitate proteins. K2CO3 (40 μL, 2 M) was added to 300 μL of the supernatant. After filtration, the sample solutions were analyzed by a Venusil MPC18 column (4.6 mm $\times$ 250 mm, 5 μm) using an HPLC system (Agilent Technologies, 1260 Infinity). The solution of 0.1 M KH_2PO_3 and methanol (95/5, V/V) were applied as the mobile phase. The flow velocity was 0.6 mL/min. The detection wavelength was 254 nm. Another fraction of the cell sample was diluted to determine the cell number using a hemocytometer, and ATP contents per cell were calculated.

2.4. Detection of mitochondrial membrane potential ($\Delta\Psi$)

The mitochondrial membrane potential ($\Delta\Psi$) was measured in live yeast by rhodamine 123 (Rho123; Beyotime, China) staining. A total of 2 $\times$ 10^6 cells were harvested by centrifugation for 3 min at 5000 rpm and room temperature and then resuspended in 1 mL of PBS. R123 was added to a final concentration of 1 μM. Following incubation in the dark for 20 min at 30 °C, the cells were washed twice with PBS and then analyzed by flow cytometry (CytoFLEX, Beckman, China). The fluorescence was detected at an excitation wavelength of 488 nm and an emission wavelength of 525 nm (FITC channel). For each sample, 10000 events were recorded, and data were reported as the mean fluorescence intensity (MFI).

2.5. Cell proliferation vitality determination (CCK-8)

Cell Counting Kit-8 (CCK-8; Beyotime, China) staining for cell proliferation was performed according to the manufacturer's instructions. Briefly, 200 μl of sample solution was seeded into 96-well plates (Costar, USA) at 800,000 cells per well with three replicates. CCK-8 solution (20 μl) was added to each well. Following incubation at 30 °C for 2 h, a microplate reader (Infinite M200, TECAN) was employed to determine the optical density (OD) at 450 nm.

2.6. Measurement of ethanol concentration

The measurement of ethanol was performed as Verduyn et al. described with modifications [29]. Stock solutions of the reagent mixture were prepared daily and kept in the dark. A reagent mixture for 100 assays consisted of 100 mL 100 mM potassium phosphate buffer (pH 7.5), to which 100 mg ABTS (2,2′-azino-di (3-ethylbenzthiazoline-6-sulfonic acid)), 150 units of commercial peroxidase, and 500 units of alcohol oxidase were added. One-milliliter aliquots of yeast cultures were centrifuged at 10,000 g and 4 °C for 3 min, and the supernatants were diluted to contain 0–200 mg/L ethanol. A 50 μl sample was added to 1 mL of reagent and mixed, and the tubes were incubated for 30 min at room temperature in the dark. The absorbance at 610 nm was measured with a UV spectrophotometer (UV-2800, UNICO, China). The ethanol content was calculated according to the standard curve established in the same way.

2.7. Measurement of glucose concentration

The Glucose (HK) Assay Kit (Sigma–Aldrich, Germany) was employed to measure the glucose concentration according to the technical bulletin. Briefly, 1 mL aliquots of yeast cultures were centrifuged at 10,000 g and 4 °C for 3 min, and the supernatants were diluted to an appropriate concentration. A 1 mL sample was added to 1 mL of reagent and mixed, and the tubes were incubated for 15 min at room temperature. The absorbance at 340 nm was measured with a UV spectrophotometer (UV-2800, UNICO, China). The

glucose content was calculated as follows:

mg glucose/mL = (ΔA) (TV) (F) (0.029)/(SV)

2.8. Measurement of oxygen consumption rate (OCR)

Yeast cells were harvested and resuspended in YPD and added to a 384-well plate that was heated to 30 °C by a plate heater. Each well contained 6×10^5 cells and a final concentration of 31.25 nM MitoXpress (Cayman, USA) probe. After being encapsulated by prewarmed heavy mineral oil (Cayman, USA) in each well, the fluorescent signal was detected by a fluorescent plate reader (FLUOstar-ACU; BMG, German).

2.9. Fluorescence microscopy

A total of 2×10^6 cells were harvested by centrifugation for 3 min at 5000 rpm and room temperature and resuspended in 1 mL of PBS. Hoechst (Hoechst 33258; Beyotime, China) was added to a final concentration of 0.5 μg/mL. Following incubation in the dark for 20 min at 30 °C, the cells were washed twice with PBS and then observed under a confocal microscope (A1R HD25; Nikon, Japan).

3. Results

3.1. DL emission of yeast cells in different growth stages

The growth phases of *S. cerevisiae* growing on glucose-based media began with a logarithmic (L) phase in the first 4 h, then

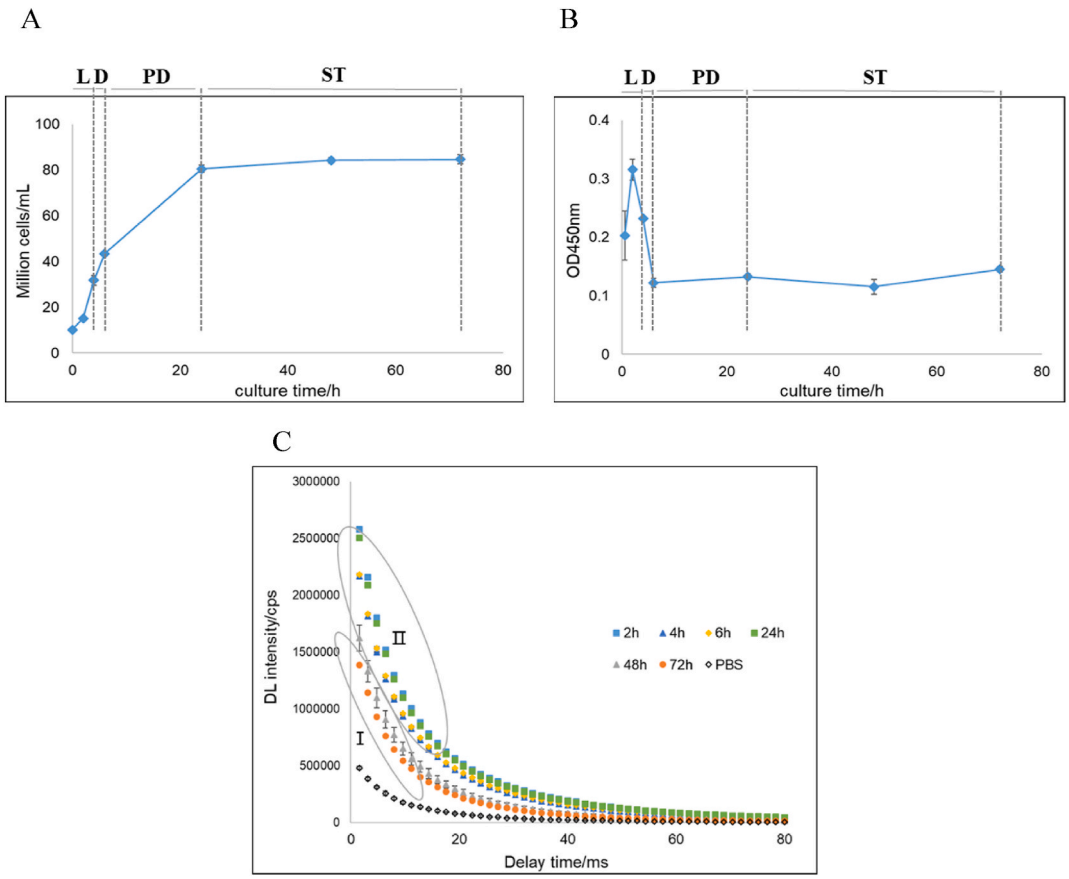

Fig. 2. Growth and DL emission of the yeast *S. cerevisiae* in different growth stages. (A) Growth kinetic curve of *S. cerevisiae*. (B) Cell proliferation viability evaluated by CCK-8 staining and OD determination at 450 nm. $p < 0.01$ at 2–4 h vs. 0 h and after 6 h. (C) DL emission kinetics curves of *S. cerevisiae* cells cultured for different times. Each curve was obtained by fitting the data to the hyperbolic function. Each sample was tested more than 5 times, and the data are presented as the means ± SEMs (n = 5). Representative experiments repeated 3 times with similar results.

progressed through diauxic (D) from 4 to 6 h and postdiauxic (PD) phases from 6 to 24 h, and finally entered into the ST phase (Fig. 2A). The cell proliferation vitality was also measured (Fig. 2B). After inoculation, yeast was cultured under conditions suitable for growth, and the high cell proliferative activity led to rapid cell proliferation between 0 and 4 h. There was a sharp decrease in cell proliferative activity in the D phase, which decreased to the lowest level and flattened in the PD and ST phases, resulting in slow cell growth between 6 and 24 h and growth arrest in the ST phase.

The trend of DL changes over time of yeast cells cultivated for different times is shown in Fig. 2C. The DL of yeast cells was maintained at approximately 80 ms or longer, and the intensity decreased monotonically with time. Meanwhile, the DL emission kinetic curves of yeast cells can be divided into two groups, and the kinetic curves of yeast cells in the ST phase of group I obviously separated from those in the L, D and PD phases (cells under growth) of group II. Although the quartz colorimetric cuvette with PBS had some DL from their own, the intensity was significantly lower than that of yeast, which did not affect the analysis of yeast DL and related parameters. Therefore, no further analysis was conducted.

The DL curves fit a hyperbolic decay function with a high fitting degree ($R^2 > 0.999$), which has been reported to be a characteristic active response of an ergodic coherent state [30]. Although fitting the DL trends by hyperbolic law originated from the analysis of experimental results, hyperbolic fitting worked so well for many biosystems that it was adopted by many authors to characterize the DL decay process [31,32]. The kinetic curve of DL intensity $I(t)$ can be modeled by a hyperbolic function as:

$$I(t) = I_0 / (1 + t/\tau)^{\beta} \quad (1)$$

And

$$\beta = \gamma/(\gamma - 1) \quad (2)$$

where I(t) is the luminescence intensity at time t after shutting off irradiation, I_0 refers to the initial DL intensity, and parameters τ and β

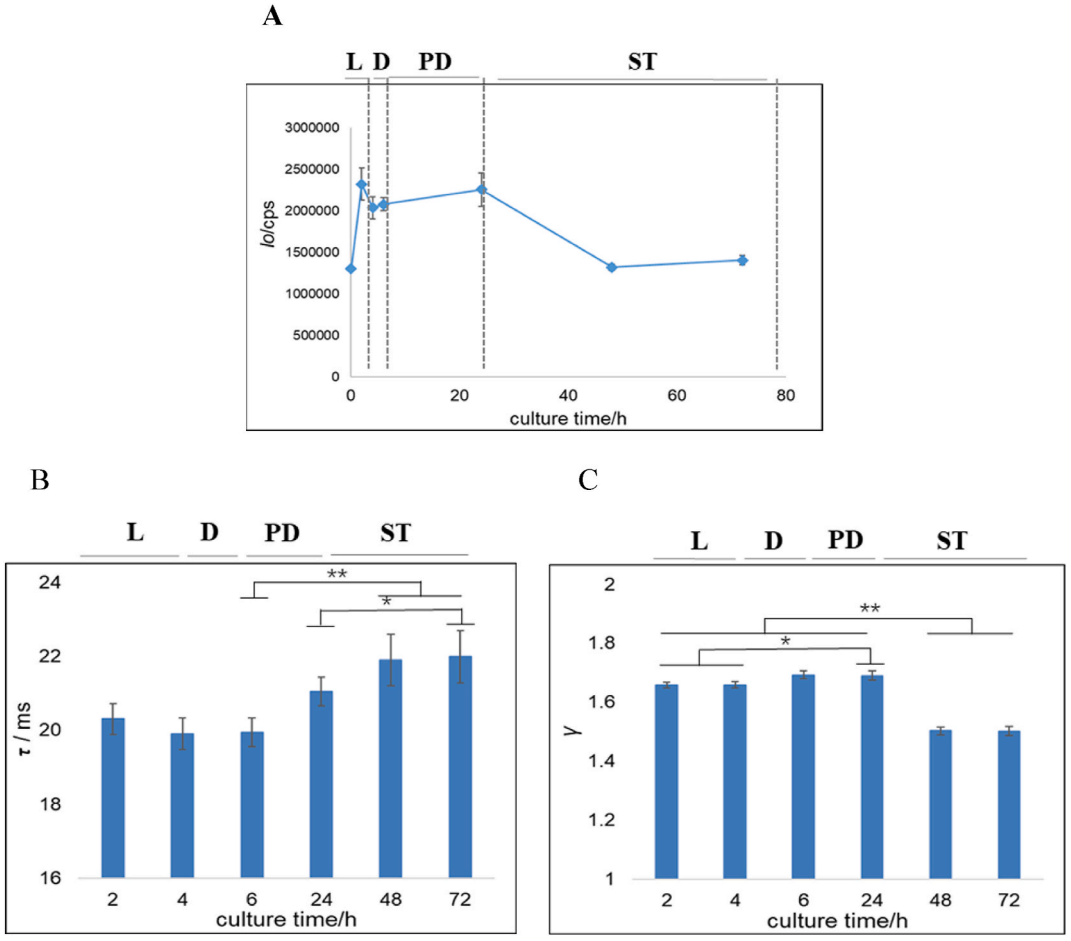

Fig. 3. DL emission parameters I_0, τ and γ of yeast cells cultured for different times. (A) Changes in I_0 of yeast cells in different phases. (B) τ values of DL emission from *S. cerevisiae* cells cultivated for different times. *$p < 0.05$, **$p < 0.01$. (C) γ values of DL emission from cells cultivated for different times. *$p < 0.05$, **$p < 0.01$. Each sample was tested more than 5 times, and the data are presented as the means ± SEMs (n = 5). Representative experiments repeated 3 times with similar results.

reflect the decay characteristics [20]. In some studies, τ and β are represented by t_0 and m or n^{-1} [33,34]. It is generally believed that I_0 and τ relate to the properties of the samples and can reflect the characteristics of the samples. According to the quantum resonant cavity theory [20], γ represents the coherence degree between molecular groups in cells. By Eq. (2), it can be evaluated as:

$$\gamma = \beta/(\beta - 1) \tag{3}$$

Based on Eqs. (1) and (3), the fitting parameters of I_0, τ and γ correlated to different characteristics of the samples were calculated. The I_0 of cells cultured for 2 h in L phase was 2,320,209 cps. Then, there was a small decrease at the end of L phase and an increase in the D and PD phases. When the cells entered the ST phase, I_0 decreased to approximately 1,400,000 cps and remained stable (Fig. 3A). The τ values of DL emission decreased gradually when the yeast cells were in the rapidly growing L and D phases and increased monotonically as the yeast cells ceased to grow in the late PD phase and ST phase. At the end of the D phase (6 h), the τ values were significantly lower than those of the ST phase cells (Fig. 3B). Similar to the I_0 changes, the γ values of DL emission of the yeast cells under growing conditions in the L, D and PD phases were significantly higher than those of the ST phase cells (Fig. 3C).

3.2. Physiological characterization of yeast cells in different growth stages

During the growth process of the yeast, glucose was consumed rapidly in the L phase and exhausted at the end of phase D, whereas ethanol was produced quickly in the L phase, remained unchanged in the D phase, consumed in the PD phase and exhausted in the later stage of the ST phase (Fig. 4A). The results showed that yeast cells grew by fermentation mode using glucose in the L phase, switched to respiratory mode in the D phase, and utilized ethanol, which was produced during the preceding fermentation stage in the PD phase. The cells ceased to grow and entered the ST phase after ethanol was exhausted. 4B shows the changes in intracellular adenosine triphosphate (ATP) levels and the cell oxygen consumption rate (OCR). In the L phase, ATP was derived primarily from glycolysis in fermentation mode, and the intracellular ATP level was significantly reduced. When cells switched to respiratory mode in D phase, the intracellular ATP level rapidly increased. Then, it decreased again in the PD and ST phases. The OCR of the D and PD phases was approximately 3–4 times that of the other phases, which was consistent with Lagunas' study on the measurement rate of oxygen consumption of yeast grown on different carbon sources [35]. The mitochondrial transmembrane potential ($\Delta\Psi$) reflects the function

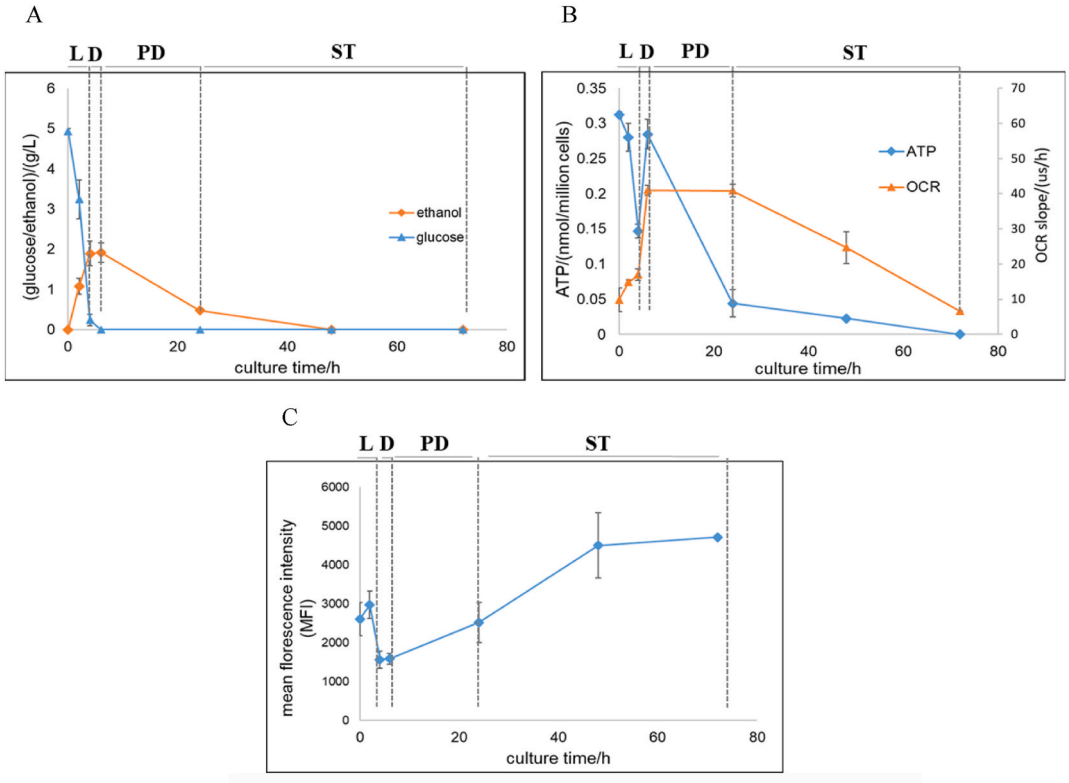

Fig. 4. The physiological characterization of the yeast *S. cerevisiae* in certain growth stages. (A) Concentration changes of glucose (Δ) and ethanol (◆) in the media. (B) ATP levels (Δ) and OCR (◆) changes in yeast cells. (C) Measurement of mitochondrial membrane potentials ($\Delta\Psi$) using fluorescent Rho123 of *S. cerevisiae* cells cultured for different times. Yeast cells were cultured for different times and harvested and stained with Rho123 for $\Delta\Psi$ determinations. MFI: mean fluorescence intensity. Each plot shows a representative experiment repeated 3 times with similar results. Data are presented as the means ± SEMs (n = 3). Abbreviations: logarithmic (L), diauxic (D), postdiauxic (PD), and stationary (ST) phases; adenosine triphosphate (ATP); oxygen consumption rate (OCR).

and state of mitochondria to a certain extent [36]. In this study, we investigated the changes in ΔΨ in yeast cells using the fluorescent probe Rho123. As shown in Fig. 4C, the mean fluorescence intensity (MFI) of cells decreased in the D phase (4 h and 6 h), which indicated a weakened permeation of the dye and promoted ΔΨ, and significantly increased in the ST phase (48 h and 72 h), which meant an enhanced permeation of the dye and reduced ΔΨ. The results suggested functional alterations in the mitochondria of yeast cells during the growth stages and the loss of ΔΨ in the ST phase.

4. Discussion

The growth phases of the yeast population growing on glucose-based media start from the L phase, pass through the D phase and PD phase, and progress to the ST phase. Since the DL kinetic curves of yeast population cells of group I (L, D and DP phases) were significantly higher than those of group II (ST phase), this provided an alternative method for discriminating the growth phase of the yeast cell population (Fig. 2C).

The DL emission parameter I_0 is an important factor that reflects the characteristics of samples and is related to the composition of the samples, biochemical reactions, excitation conditions, and other factors [12]. In this study, yeast cells entered the L phase with rapid growth after inoculation in glucose-containing medium. In the first 2 h, yeast cells regulated mitochondrial function (the MFI of Rho123 increased slightly, Fig. 4C) and grew through fermentation of the available glucose accompanied by a decrease in the intracellular ATP level and a slight increase in the cell OCR (Fig. 4B). The DL emission detection results showed that I_0 increased significantly during this adjustment process. From 2 to 4 h, due to sufficient glucose in the medium (Fig. 4A), yeast cells continued to produce ethanol, mitochondria functioned well (high ΔΨ), and I_0 decreased slightly. As glucose became a limiting factor at the end of exponential growth, yeast shifted their metabolic state from one that favors fermentation to one that favors respiration [37]. Consequently, yeast cells shift their metabolism from a state conducive fermentation to a state conducive to respiration in the D and PD phases, the intracellular ATP level and OCR of the cells increase significantly, and I_0 increases again. When yeast cells entered the ST phase, the cells ceased to grow, and a loss of ΔΨ was observed. At the same time, I_0 significantly decreased during this period. Consequently, we believed that I_0 fluctuated with metabolic pathway conversion and cell growth and was to some extent related to the mitochondria and cell state.

Another important parameter of DL emission is τ, which represents the coherence time of biomolecules in the biosystem [20,38]. The larger τ *is*, the slower the DL decays. Gu inferred that τ revealed the degree of order of the biosystem, and his research showed that τ declined along with the decrease in pear freshness [20]. In his opinion, a larger τ represented a longer coherence time between molecules in an organism, which meant a higher degree of order and a lower entropy in the biological system. In a study by Lanzanò L. [33], τ values evaluated by a modified hyperbolic function showed a monotonic decrease as a function of age as well. In our study, the τ values of ST phase cells were significantly higher than those of growing cells during the growth stages of the yeast cell population (Fig. 3B), indicating that the coherence time of the ST phase cells was longer. According to the quantum resonant cavity theory [20], γ *r*epresents the coherence degree between molecular groups in cells. The γ value of growing cells was significantly higher than that of ST phase cells (Fig. 3C), indicating a higher coherence degree between molecular groups in growing cells. Combining τ and γ, we hypothesized that the higher the coherence degree (γ) between molecular groups, the higher the order and the lower entropy of the biological system, the faster the restoration of the biological system to its initial state after photoexcitation, and the shorter the coherence time (τ) of the DL emission. Although there are some differences, we think that both τ and γ of DL emission are important parameters to reveal the characteristics of samples, and our study contributes to a better understanding of DL emission, providing a new perspective for related research.

To date, the origin of DL is still under debate, but it is generally believed that DL may originate from a variety of possible reactions and sources in biological systems. Our study revealed that DL emission from yeast cells can indirectly reflect the cell metabolic and growth state. DL has been widely used to distinguish normal cells from cancer cells [11–13]. Owing to the energy metabolic similarities between tumor cells and yeast, yeast cells are commonly used as an experimental model for cancer research [39]. The changes in DL emission parameters in yeast cells during energy metabolic pathway transformation may provide new ideas for cancer research. Meanwhile, the study of the yeast stationary phase provides important insights into the mechanisms of aging in other organisms [40,41]. Therefore, the DL emission differences between yeast growing cells and ST phase cells may provide another method for monitoring cell aging and require more in-depth research.

In conclusion, in this work we have taken the first step toward using DL to monitor the growth stages of the yeast *S. cerevisiae* growing on glucose-based media. The DL emission kinetics curve can be used as an alternative method for the identification of yeast cell populations during different growth periods. The DL emission parameters of I_0, τ and γ can reflect some characteristics of the growth stages of yeast cells to a certain extent and may be an optional entropy evaluation method, which provides a wider application prospect for this technology.

Data availability statement

Data included in article/supp. material/referenced in article.

CRediT authorship contribution statement

Qing Li: Writing – review & editing, Writing – original draft, Validation, Supervision, Project administration, Methodology, Investigation, Formal analysis, Data curation, Conceptualization. **Hong Wu:** Supervision, Project administration, Conceptualization.

Miao Tian: Methodology, Investigation. **Danyu Li:** Methodology, Investigation. **Peng Zheng:** Software. **Xiaochun Zhang:** Software, Methodology. **Bruce Qing Tang:** Validation, Supervision, Resources, Funding acquisition.

Declaration of competing interest

The authors declare that they have no known competing financial interests or personal relationships that could have appeared to influence the work reported in this paper.

Acknowledgments

We sincerely thank Yanjie Chen for the ATP measurement, and this work was supported by the ENN Research Fund.

References

[1] M. Cifra, C. Brouder, M. Nerudová, et al., *J LUMIN.* Biophotons, coherence and photocount statistics, Acritical review 164 (2015) 38–51, https://doi.org/10.1016/j.jlumin.2015.03.020.
[2] A. Scordino, I. Baran, M. Gulino, et al., *J PHOTOCH PHOTOBIO B.* Ultra-weak delayed luminescence in cancer research: a review of the results by the ARETUSA equipment 139 (2014) 76–84, https://doi.org/10.1016/j.jphotobiol.2014.03.027.
[3] L.J.J. Kricka, BIOLUMIN CHEMILUMIN, Light emission by plants and bacteria 2 (2) (1988) 112, https://doi.org/10.1002/bio.1170020209.
[4] B.L. Strehler, W. Arnold, Light Production by Green Plants, vol. 34, 1951, pp. 809–820, https://doi.org/10.1085/jgp.34.6.809.
[5] B.L. Strehler, ARCH BIOCHEM BIOPHYS. The luminescence of isolated chloroplasts 34 (1951) 239–248, https://doi.org/10.1016/0003-9861(51)90001-X.
[6] W. Arnold, J. Thompson, *J GEN PHYSIOL.* Delayed light production by blue-green algae, red algae, and purple bacteria 39 (1956) 311–318, https://doi.org/10.1085/jgp.39.3.311.
[7] H.J. Niggli, S. Tudisco, G. Privitera, et al., Laser-ultraviolet-A induced ultraweak photon emission in mammalian cells, BIOPHOTONICS 10 (2) (2005) 024006, https://doi.org/10.1007/0-387-24996-6_14.
[8] H.J.J. Niggli, P. Photoch, Artificial sunlight irradiation induces ultraweak photon emission in human skin fibroblasts 18 (2–3) (1993) 281–285, https://doi.org/10.1016/1011-1344(93)80076-L.
[9] L. Lanzanò, R. Grasso, M. Gulino, et al., *INDIAN J EXP BIOL.* Corresponding Measurements of Delayed Luminescence and Impedance Spectroscopy on Acupuncture Points, vol. 46, 2008, pp. 364–370. PMID: 18697621.
[10] F. Musumeci, L.A. Applegate, G. Privitera, et al., *J PHOTOCH PHOTOBIO B.* Spectral analysis of laser-induced ultraweak delayed luminescence in cultured normal and tumor cells: temperature dependence 79 (2) (2005) 93–99.
[11] F. Musumeci, G. Privitera, A. Scordino, et al., Discrimination between normal and cancer cells by using spectral analysis of delayed luminescence, Appl. Phys. Lett. 86 (15) (2005) 153902, https://doi.org/10.1063/1.1900317.
[12] P. Chen, L. Zhang, F. Zhang, et al., *BIOMED OPT EXPRESS.* Spectral discrimination between normal and leukemic human sera using delayed luminescence 3 (2012) 1787–1792, https://doi.org/10.1364/BOE.3.001787.
[13] H.W. Kim, S.B. Sim, C.K. Kim, et al., *CANCER LETT.* Spontaneous photon emission and delayed luminescence of two types of human lung cancer tissues: Adenocarcinoma and Squamous cell carcinoma 229 (2) (2005) 283–289.
[14] A. Scordino, A. Campisi, R. Grasso, et al., *J BIOMED OPT.* Delayed luminescence to monitor programmed cell death induced by berberine on thyroid cancer cells 19 (11) (2014) 117005, https://doi.org/10.1117/1.JBO.19.11.117005.
[15] I. Baran, C. Ganea, S. Privitera, et al., *OXID MED CELL* LONGEV. Detailed analysis of apoptosis and delayed luminescence of human Leukemia Jurkat T Cells after proton irradiation and treatments with oxidant agents and flavonoids 2012 (2012) 498914, https://doi.org/10.1155/2012/498914.
[16] I. Baran, C. Ganea, A. Scordino, et al., *CELL BIOCHEM BIOPHYS.* Effects of menadione, hydrogen peroxide, and quercetion apoptosis and delayed luminescence of human Leukemia Jurkat, T-Cells 58 (2010) 169–179, https://doi.org/10.1007/s12013-010-9104-1.
[17] M.N. Jamaludin, Balakrishnan M. Jurnal Teknologi, Development of spectral delayed luminescence system for whole saliva analysis: a prototype study 67 (1) (2014) 7–14.
[18] F. Musumeci, L. Lanzanò, S. Privitera, et al., PROC SPIE. Spectral analysis of photoinduced delayed luminescence from human skin, 66331K-66331K-8 6633 (2007), https://doi.org/10.1117/12.727696.
[19] U. Lucia, A. Physica, Entropy Generation Approach to Cell Systems, vol. 406, 2014, pp. 1–11.
[20] Q. Gu, Biophotonics, third ed., Science Press, 2016.
[21] P.K. Herman, CURR OPIN MICROBIOL. Stationary phase in yeast 5 (2002) 602–607, https://doi.org/10.1016/S1369-5274(02)00377-6.
[22] A.A. Goldberg, S.D. Bourque, P. Kyryakov, et al., *EXP GERONTOL.* Effect of calorie restriction on the metabolic history of chronologically aging, Yeast 44 (9) (2009) 555–571, https://doi.org/10.1016/j.exger.2009.06.001.
[23] J. Slawinski, A. Ezzahir, M. Godlewski, et al., *EXPERIENTIA.* Stress-Induced Photon Emission from Perturbed Organisms, vol. 48, 1992, pp. 1041–1058, https://doi.org/10.1007/BF01947992.
[24] I. Baran, C. Ganea, I. Ursu, et al., *ROM J PHYS.* Effects of nocodazole and ionizing radiation on cell proliferation and delayed luminescence 54 (5) (2009) 557–567.
[25] Q. Li, M. Tian, Y. Liu, et al., *GEN PHYSIOL BIOPHYS.* Delayed luminescence as a tool for detecting oxidative stress in Saccharomyces cerevisiae 41 (1) (2022) 79–86, https://doi.org/10.4149/gpb_2021042.
[26] M. Tian, Q. Li, Y. Liu, et al., Relationship between DL emission and mitochondrial status in Saccharomyces cerevisiae 12 (2022) 394, https://doi.org/10.1038/s41598-021-04290-9.
[27] Q. Li, M. Tian, J. Teng, et al., Radio frequency–induced superoxide accumulationaffected the growth and viability of Saccharomyces cerevisiae 23 (2020) 391–396, https://doi.org/10.1007/s10123-019-00111-2.
[28] Y. Sumi, T. Woehrle, Y. Chen, et al., *SHOCK.* Plasma ATP is required for neutrophil activation in a mouse sepsis model 42 (2) (2014) 142–147, https://doi.org/10.1097/SHK.0000000000000180.
[29] C. Verduyn, J.P. van Dijken, W.A.J. Scheffers, M.E.T.H. Microbiol, Colorimetric alcohol assays with alcohol oxidase 2 (1) (1984) 15–25, https://doi.org/10.1016/0167-7012(84)90027-7.
[30] F.A. Popp, Y. Yan, L.E.T.T.A. Phys, Delayed Luminescence of Biological System in Terms of Coherent States, vol. 293, 2002, pp. 93–97. 10.1016/S0375-9601(01)00831-3.
[31] M.M. Sun, W.T. Chang, E.V. Wijk, et al., *CHIN MED.* Application of delayed luminescence method on measuring of the processing of Chinese herbal materials 13 (1) (2018), https://doi.org/10.1186/s13020-018-0202-0.
[32] G. Palazzo, A. Mallardi, A. Hochkoeppler, , et al.J. Biophys, Electron transfer kinetics in photosynthetic reaction centers embedded in trehalose glasses: trapping of conformational substates at room temperature 82 (2) (2002) 558–568, https://doi.org/10.1016/S0006-3495(02)75421-0.
[33] L. Lanzanò, A. Scordino, S. Privitera, et al., Spectral analysis of delayed luminescence from human skin as a possible non-invasive diagnostic tool, Eur. Biophys. J. 36 (2007) 823–829, https://doi.org/10.1007/s00249-007-0156-0.

[34] H. Bai, P. Chen, L. Lin, et al., PROC SPIE. Physical mechanism of delayed luminescence from human serum 7182 (2009) 71820K, https://doi.org/10.1117/12.808875.
[35] R. Lagunas, Bba-Bioenergetics, Energy metabolism of Saccharomyces cerevisiae discrepancy between ATP balance and known metabolic functions 440 (3) (1976) 661–674, https://doi.org/10.1016/0005-2728(76)90049-9.
[36] B. Kavakçıoğlu, L. Tarhan, *ARCH MICROBIOL*. Yeast caspase-dependent apoptosis in Saccharomyces cerevisiae BY4742 induced by antifungal and potential antitumor agent clotrimazole 200 (1) (2018) 97–106, https://doi.org/10.1007/s00203-017-1425-7.
[37] M. Kaeberlein, C.R. Burtner, B.K. Kennedy, *PLOS GENET*. Recent developments in, yeast aging 3 (5) (2007) e84, https://doi.org/10.1371/journal.pgen.0030084.
[38] Q. Gu, On Coherence Theory of Biophoton Emission, vol. 5, 1999, pp. 17–20.
[39] R. Diaz-Ruiz, S. Uribe-Carvaja, A. Devin, et al., *BBA-REV CANCER*. Tumor cell energy metabolism and its common features with yeast metabolism 1796 (2) (2009) 252–265, https://doi.org/10.1016/j.bbcan.2009.07.003.
[40] V.D. Longo, *NEUROBIOL AGING*. Mutations in signal transduction proteins increase stress resistance and longevity in yeast, nematodes, fruit flies, and mammalian neuronal cells 20 (5) (1999) 479–486, https://doi.org/10.1016/S0197-4580(99)00089-5.
[41] M. MacLean, N. Harris, Piper P.W. Yeast, Chronological lifespan of stationary phase yeast cells; a model for investigating the factors that might influence the ageing of postmitotic tissues in higher organisms 18 (6) (2001) 499–509, https://doi.org/10.1002/yea.701.